

## ELECTRONIC STATES OF 1,3,5-SYM-TRIAZINE. II. GEOMETRY OF THE ${}^1E''$ AND ${}^3E''$ STATES IN THE CRYSTAL†\*

E.R. BERNSTEIN and R.E. SMALLEY††

*Department of Chemistry, Princeton University, Princeton, N.J. 08540, USA  
and Francis Bitter National Magnet Laboratory\*\*, Massachusetts Institute of Technology,  
Cambridge, Massachusetts 02139, USA*

Received 20 August 1973

Through Stark, Zeeman, Zeeman-Stark, and absorption spectra of  $h_3$ ,  $h_2d_1$ ,  $h_1d_2$ , and  $d_3$ -sym-triazine isotopes it has been determined that the lowest observed singlet-singlet transition ( ${}^1E'' \leftarrow {}^1A'_1$ , assigned in the gas phase) and singlet-triplet transition ( ${}^3E'' \leftarrow {}^1A'_1$ , predicted experimentally and theoretically) of this molecule are both crystal field split by at least ca  $200\text{ cm}^{-1}$  in the low temperature monoclinic crystal. The observed sharp crystal origins for singlet and triplet regions are assigned to transitions involving one component of the split  ${}^1E''$  and  ${}^3E''$  excited states, respectively. From  $h_2d_1$ , and  $h_1d_2$ -sym-triazine absorption intensity ratios for these transitions, it has been demonstrated that the excited state geometry is "quinoidal" (i.e., four long and two short bonds) at  $4.2^\circ\text{K}$  in each excited state.

### I. Introduction

Surprisingly little is known about the excited electronic states of sym-triazine considering its size, apparent simplicity, high symmetry, and importance as a prototype molecule for aromatic azines. The fact that sym-triazine has a complex and highly forbidden low lying gas phase spectrum, degenerate ( $E''$ )  $S_1$  and  $T_0$  excited states, a low temperature triply-twinned crystal phase, and a dense excited electronic manifold has made this a particularly difficult system to study and understand. These complications, however, render sym-triazine especially interesting and important in terms of molecular electronic spectroscopy of medium size molecules and molecular crystals.

In part I of this series [1] results were presented concerning optical absorption spectra of pure, isotopic, and chemical mixed crystals of sym-triazine at  $4.2^\circ\text{K}$ . The lowest observed singlet-triplet transition (region I:  $T_0 \leftarrow S_0$ ) and the lowest observed singlet-singlet transition (region II:  $S_1 \leftarrow S_0$ ) for the  $C_{2v}$  symmetry isotopes  $d_2h_1$ - and  $d_1h_2$ -sym-triazine were found to split by 30 and  $25\text{ cm}^{-1}$ , respectively. For both these features, on the other hand,  $D_{3h}$  symmetry isotopes  $h_3$ - and  $d_3$ -sym-triazine give single absorption lines ( $1-3\text{ cm}^{-1}$  fwhh). Using these data in conjunction with published results of earlier workers [2-8]\*, arguments were presented which led to assignment of these transitions as  ${}^3E'' \leftarrow {}^1A'_1$  (region I) and  ${}^1E'' \leftarrow {}^1A'_1$  (region II).

In this second paper on sym-triazine we present Zeeman, Stark-Zeeman, and Stark experiments which were designed to test the hypothesis that these transitions involve orbitally degenerate excited states in the low temperature ( $< 213^\circ\text{K}$ ) crystal. In the process the geometry of sym-triazine in the low temperature monoclinic crystal phase has been ascertained.

† This work was reported at The 28th Symposium on Molecular Structure and Spectroscopy, The Ohio State University, June 11-15, 1973 (see abstract 12).

\* Supported in part by the U.S. Army Research Office, (Durham), The Office of Naval Research, and The National Science Foundation.

†† Princeton University Harold W. Dodds Fellow, 1972-73; present address: James Franck Institute, University of Chicago, Chicago, Illinois 60637, USA.

\*\* Supported by the National Science Foundation.

\* See, however, Note added in proof, of ref. [1].

## 2. Experimental

### 2.1. Crystal preparation

Zeeman and Stark experiments were performed on crystals grown from the melt at a rate of 1 cm/day by conventional Bridgman techniques. Deuterated sym-triazines were synthesized in vacuo by methods described in I.  $h_3$ -sym-triazine was obtained from commercial sources and purified as previously described. Crystals were cut, oriented, and polished at room temperature and were subsequently cooled to 77°K over a period of about 12 hours [9]. Optical quality of these samples at 4.2°K was not particularly good due to room temperature crystal imperfections (micro-cracks) exaggerated and amplified by stresses induced by the triple-twinning which accompanies the phase transition at 213°K [10].

### 2.2. Zeeman apparatus

Zeeman experiments were carried out at the Francis Bitter National Magnet Laboratory (NML) using a conventional split-core Bitter magnet capable of fields up to 100.5 kG. The magnet bore was sufficiently large to allow samples of up to 2 cm in length to be mounted in liquid helium in a magnetic field that was homogeneous to better than 1% over the entire sample volume. A 2 m Bausch and Lomb spectrograph was used to record absorption spectra photographically at a dispersion of 2 Å/mm. All Zeeman data were taken with  $H$  perpendicular to the propagation direction of the monitoring light beam. The magnetic field was calibrated by the staff of NML and was found to be constant for the duration of experiments reported below.

### 2.3. DC Stark apparatus

Stark data were obtained with single crystals mounted between two highly polished, parallel, stainless steel electrodes. It was soon discovered in the course of these experiments that whenever the sample was not in good and direct contact with both electrodes, observed dc Stark splittings were highly variable. This effect is probably due to build-up of charge on the surface of the sample when "blocking electrodes" are employed. The time dependence of a Stark splitting

can be so severe as to cause the splitting to be reduced by a factor of two over a period of one-half hour. The initially observed Stark splitting pattern may be regained by reversing the applied field. The mechanism of this charge build-up is not well understood. Careful filtering of light used to measure the absorption spectrum was found to have little if any effect.

All dc experiments reported here, however, were performed with samples in good contact with both electrodes. These experiments yielded highly reproducible ( $\pm 0.2 \text{ cm}^{-1}$ ) Stark splitting which were time independent and varied smoothly and monotonically with field strength. Stark spectra were recorded on a McPherson 2 m  $f/17$  Czerny-Turner spectrograph with corrected optics. Typically this instrument was used in 2nd or 3rd order of a 1200 groove/mm grating (blazed at 7500 Å) at a dispersion of 1.8 or 1.2 Å/mm, respectively. Spectra were recorded on Kodak 103a-0 plates as well as photoelectrically with a RCA 8850 photomultiplier tube operated in the photon counting mode [9].

## 3. Experimental results

### 3.1. Zeeman experiments

Fig. 1 shows the absorption spectrum in region I of a 2 cm long single crystal of  $d_3$ -sym-triazine oriented such that  $H$  makes an angle of less than 30° with respect to the crystallographic (low temperature)  $c$  axis. There are no indications of any splitting of the high field Zeeman pattern into more than three lines, to within the spectral slit width of  $0.4 \text{ cm}^{-1}$ . Patterns for  $H$  parallel and perpendicular to  $c$  were always found to be identical in all respects to those obtained by direct extrapolation of earlier low field work [4, 5] to  $|H| = 100.5 \text{ kG}$ . At maximum field values the center line of the triplet pattern is within  $0.2 \text{ cm}^{-1}$  of the pattern mid-point. The  $g$  value is isotropic and equal to  $1.93 \pm 0.1$ .

A 2 cm long crystal of  $d_3$ -sym-triazine was prepared containing  $\sim 15\%$   $^{13}\text{C}_3$ -sym-triazine\*. Fig. 2 presents high field Zeeman results on this crystal in

\* In I is described a synthesis of sym-triazine from starting materials with a H:D ratio of 1:1. The sym-triazine synthesized from this mixture has an isotope ratio of 1:3:3:1. The mnemonic used for this material is  $^{13}\text{C}_3$ -sym-triazine.

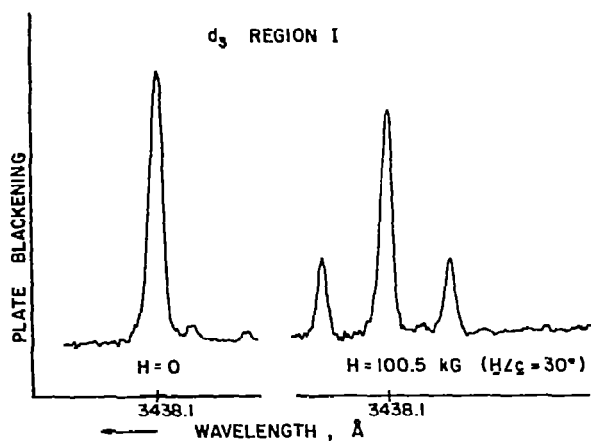


Fig. 1. Region I absorption spectrum of a 2 cm long crystal of  $d_3$ -sym-triazine at  $4.2^\circ\text{K}$  and at zero and 100.5 kG. For this experiment  $k$  (propagation vector of the monitoring light beam) was perpendicular to the applied magnetic field,  $H$  and the crystal  $c$  axis, and  $H \perp c \sim 30^\circ$ . The measured  $g$  value from this plate was  $1.93 \pm 0.1$ .

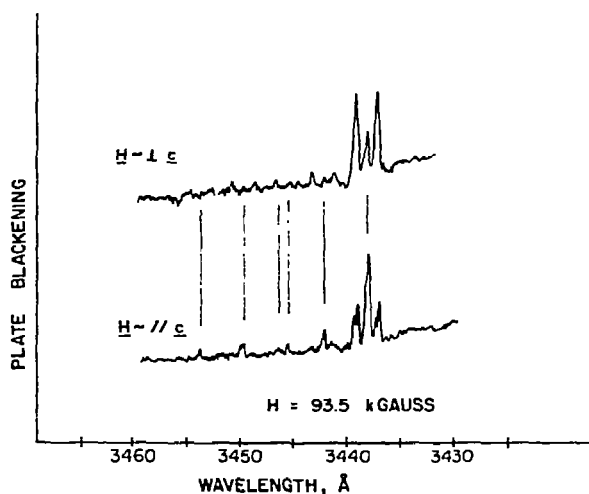


Fig. 2. Region I 93.5 kG absorption spectrum of a 2 cm long  $d_3$ -sym-triazine crystal containing  $\sim 15\%$   $1331$ -sym-triazine at  $4.2^\circ\text{K}$ . In these experiments  $k \perp H, c$  and  $H \perp c$  or  $H \parallel c$  as indicated. The pronounced structure on the red side of each line is due to guest-guest and guest-host perturbed features arising from the heavy loading of isotopic impurities in this sample.

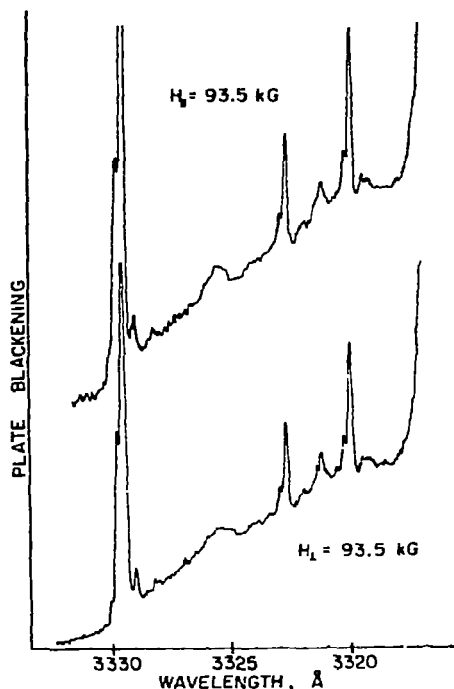


Fig. 3. Region II 93.5 kG absorption spectra of a 5 mm  $d_3$ -sym-triazine crystal doped with  $\sim 4\%$   $h_3$ -sym-triazine at  $4.2^\circ\text{K}$ . In these experiments  $k \perp H, c$  and  $H \parallel c$  or  $H \perp c$  as indicated. Again, red guest-guest perturbed features are evident.

region I with  $H \parallel c$  and  $H \perp c$ . High field spectra are complicated by red host-guest and guest-guest perturbed absorption features present at zero field [1, 9]. Zeeman patterns for *all* lines of all isotopes are identical for region I.

On the same exposures used to record the spectra of  $d_3$ -sym-triazine as presented in figs. 1 and 2, region II ( $S_1 \leftarrow S_0$ ) absorptions of  $d_2h_1$ -,  $h_2d_1$ -, and  $h_3$ -sym-triazine species were also obtained. No evidence was observed in these experiments for any Zeeman effect whatsoever on region II absorptions - including  $D_{3h}$  symmetry species. The spectral slit width in these experiments was  $0.4 \text{ cm}^{-1}$ . Fig. 3 presents the results of a 100.5 kG ( $H \parallel c$  and  $H \perp c$ ) Zeeman experiment on region II absorptions of a  $d_3$ -sym-triazine sample which was doped with 4%  $h_3$ -sym-triazine. While the region I ( $T_0 \leftarrow S_0$ ) transition of this crystal showed perfect  $H \parallel c$  and  $H \perp c$  Zeeman patterns, again, absolutely no Zeeman effects (either splittings or broad-

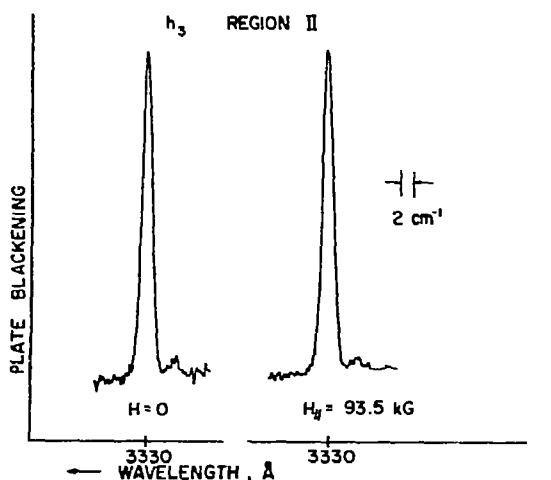


Fig. 4. Region II absorption spectra of 0.5 mm  $h_3$ -sym-triazine crystal at zero and 93.5 kG ( $H \parallel c$ ) at 4.2° K. Careful examination of the photographic plates from which this data was drawn reveals no indication of any effect of the magnetic field upon the region II absorption line.

enings) were observed on any of the region II absorption lines. Fig. 4 gives a similar densitometer trace of a photographic plate obtained with  $H \parallel c$  in region II on a 0.5 mm thick  $h_3$ -sym-triazine crystal.

Thus it appears that the large region II Zeeman splitting reported by Hochstrasser and Zewail [4]\* does not exist. Line shape analyses of high field Zeeman data, when compared to zero field line shapes, indicate that the maximum undetectable  $g$  value is no larger than 0.04.

The recent Zeeman experiments of Aartsma and Wiersma [12] confirm the above findings.

### 3.2. Stark-Zeeman experiments

Crossed field dc Stark-Zeeman experiments were performed on region I. Fig. 5 gives a region I absorption spectrum of a 13 × 7 × 1.8 mm  $h_3$ -sym-triazine single crystal with  $H \parallel c \perp E$ . The vectors  $H$ ,  $E$ , and  $c$

\* The 1.33  $\text{cm}^{-1}$  splitting at 55 kG, as reported in [4], gives  $g = 0.52$ . Recent results obtained by Hochstrasser and Zewail [11] give a value of  $g = 0.11 \pm 0.08$ . The error quoted is one standard deviation; measurements were performed photoelectrically at 4.2° K with a superconducting magnet.

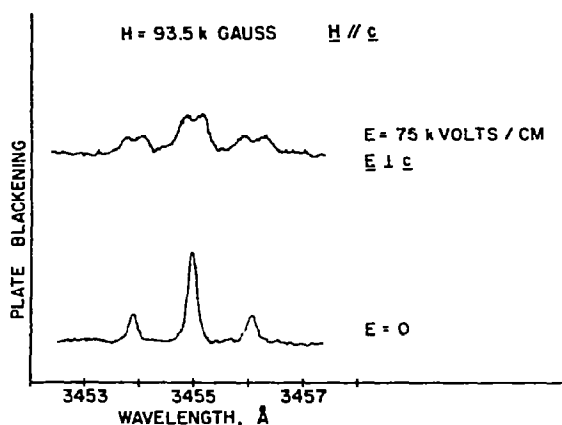


Fig. 5. DC Stark-Zeeman experiment on the region I absorption of a 13 × 7 × 1.8 mm crystal of  $h_3$ -sym-triazine at 4.2° K. In this experiment  $k \perp H$ ,  $E$ ,  $c$ ;  $H \parallel c \perp E$ .

were perpendicular to  $k$  (propagation vector of the monitoring light beam) and  $k$  was parallel to the long axis of the crystal. The sample was in contact with both electrodes even at low temperature. At maximum attainable electric field strengths (75 kV/cm) all three Zeeman absorption lines are split by  $\sim 2.6 \text{ cm}^{-1}$ , in excellent agreement with previously reported Stark data at  $H = 0$  for region I of  $h_3$ -sym-triazine [8]. This two-field experimental result is then a simple superposition of independent Zeeman and Stark perturbations.

### 3.3. Stark experiments

Fig. 6 presents results of a dc Stark experiment on region II absorptions of a  $d_3$ -sym-triazine crystal containing  $\sim 3\%$   $d_2h_1$ -sym-triazine and  $\sim 4\%$   $h_3$ -sym-triazine. With  $\vec{E} \perp c$  at an 84 kV/cm field strength, all region II features show exactly the same Stark splittings for all isotopes. Note especially both components of the  $C_{2v}$  isotope are split. Splittings are all  $3.6 \pm 0.2 \text{ cm}^{-1}$ , again in agreement with  $h_3$ -sym-triazine data of ref. [8].

On close inspection, high field patterns appear to be considerably broader than one might expect based on a simple splitting of zero field lines in a homogeneous electric field. To explore this apparent discrepancy more fully a new sample (grown at 0.9 cm/day from the melt) was carefully oriented, cut, and polished.

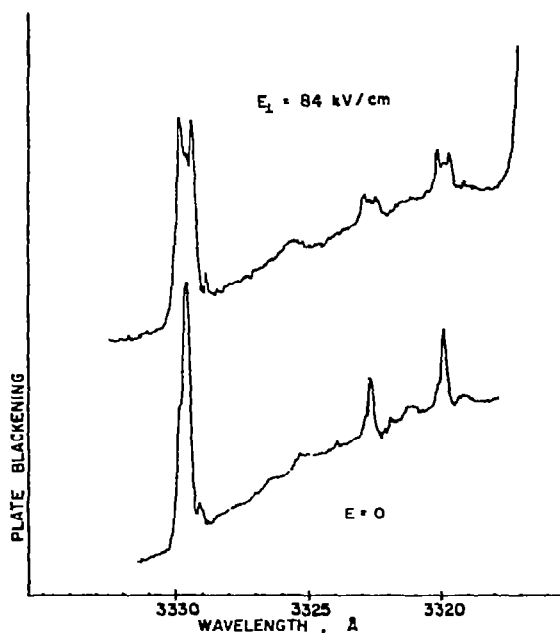


Fig. 6. DC Stark experiment on the region II absorption spectrum of a 8 mm  $d_3$ -sym-triazine crystal doped with  $\sim 4\%$   $h_3$ -sym-triazine. In this experiment  $E \perp c$  and  $E, c \perp k$ .

The resultant crystal had the shape of a rectangular parallelepiped 2.9 mm thick by 7 mm long by 5 mm high. The  $c$  axis was along the vertical direction ( $\pm 5^\circ$ ), and crystal thickness was uniform to  $\pm 0.05$  mm. This single crystal was mounted between two 2.5 cm square stainless steel electrodes. The assembly was clamped in a teflon holder such that there was intimate and even contact with both electrodes over the 7 mm X 5 mm surfaces. The electrodes were measured to be parallel to better than  $\pm 0.05$  mm at 300°K. This measurement was repeated on the cold sample mount (dripping liquid air) after the spectroscopic experiment was completed; electrodes were found to have retained their parallelism and good contact with the sample.

Even with enough care to eliminate electric field inhomogeneities, the region I high field splitting pattern for this setup was considerably broader than what would be expected for a simple splitting of the zero field line (see fig. 7). Fig. 8 depicts a best fit to the observed  $E_\perp = 70$  kV/cm splitting pattern with two half intensity  $E = 0$  lines separated by an appropriate amount. The line width discrepancy is quite clear.

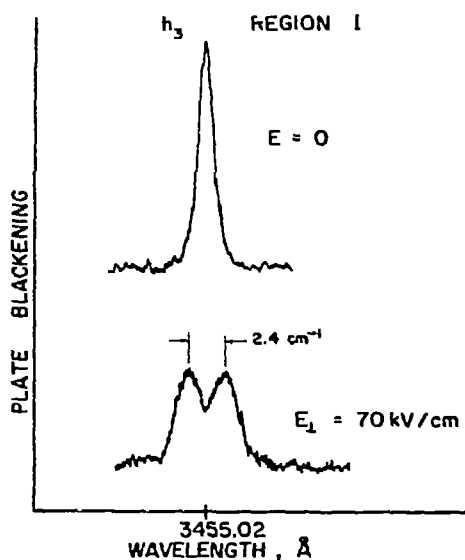


Fig. 7. DC Stark results on the region I absorption of a 7 mm crystal of  $h_3$ -sym-triazine at 4.2°K.  $E \perp c$ ;  $E, c \perp k$ . Photographic data.

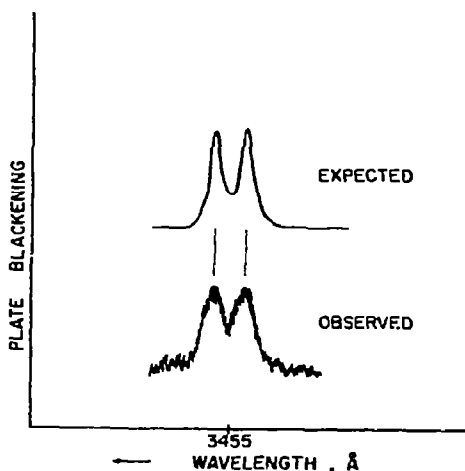


Fig. 8. Best fit to high field 2 line Stark pattern with simply split zero field gaussian lines of appropriate zero field width.

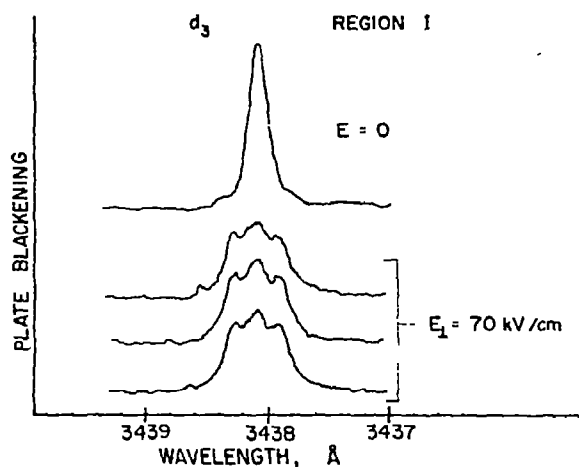


Fig. 9. DC Stark results on the region I absorption of a 8 mm  $d_3$ -sym-triazine crystal which contained  $\sim 2\%$   $h_3$ -sym-triazine and  $\sim 3\%$   $d_2h_1$ -sym-triazine.  $E \perp c$ ;  $E, c \perp k$ ;  $T = 4.2^\circ\text{K}$ . Three independent tracings of different areas of the same exposure are presented in the high field case.

Another sample, specifically designed to investigate and document this broadening phenomenon in region II, was prepared from highly purified  $h_3$ -sym-triazine to which had been added  $\sim 2\%$   $h_3$ -sym-triazine. The boule was simultaneously grown with the sample discussed immediately above in the same Bridgman furnace. A crystal was oriented, cut, polished, mounted, and cooled to  $4.2^\circ\text{K}$  in exactly the same manner as the previous  $h_3$  sample. Fig. 9 is a densitometer tracing of the high field ( $E_1 = 70 \text{ kV/cm}$ ) Stark pattern obtained for this sample; this three maxima pattern is for the  $d_3$ -sym-triazine host  $T \leftarrow S_0$  absorption. Fig. 10 presents an identical absorption structure simultaneously observed for region II ( $S_1 \leftarrow S_0$ ) for the  $2\%$   $h_3$ -sym-triazine guest. Fig. 11 gives this same three component pattern on both region II features of  $d_2h_1$ -sym-triazine. As was the case previously, this isotopic mixed crystal was in full and even contact with electrodes throughout this experiment. Again the cold electrodes were measured, after the experiment, to be parallel to better than  $\pm 0.05 \text{ mm}$ . During the course of all these experiments, magnitude of the field applied to the electrodes was observed to be constant to within our ability to measure it ( $\pm 2\%$ ).

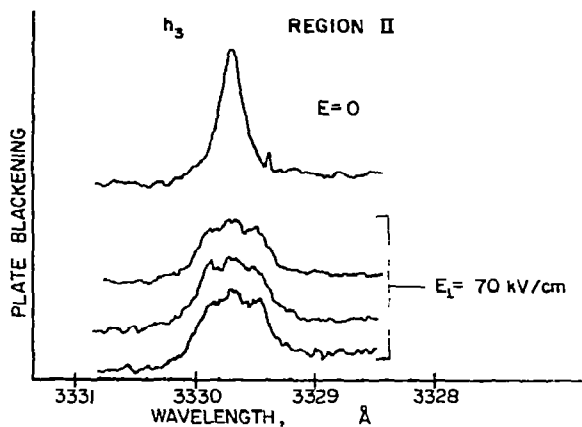


Fig. 10. DC Stark results of the region II absorption of the  $h_3$ -sym-triazine species in a crystal of  $d_3$ -sym-triazine. These microdensitometer traces were taken from the same exposure used for figs. 9 and 11.

#### 4. Discussion

In I it was argued that region II absorption was due to  ${}^1E'' \leftarrow {}^1A_1$  and region I absorption, based on the almost perfect one to one correspondence of  $C_{2v}$  and  $D_{3h}$  absorption data for both features, was assigned as  ${}^3E'' \leftarrow {}^1A_1$ . These crystal assignments were made primarily because published Zeeman results [4] on

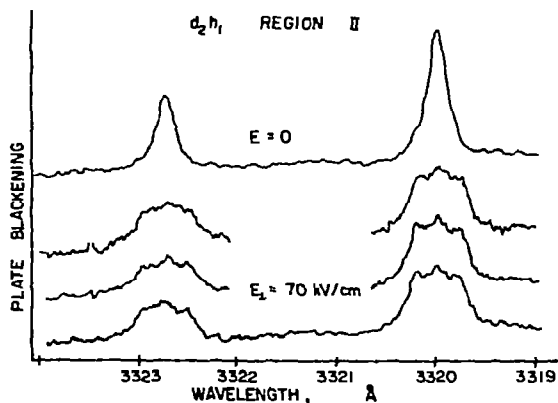


Fig. 11. DC Stark results on the region II absorption of the  $d_2h_1$ -sym-triazine species in a  $d_3$ -sym-triazine crystal. These microdensitometer traces were taken from the same exposures used for figs. 9 and 10.

region II demanded that  $\langle L_z \rangle \neq 0$ ; that is, the excited state was orbitally degenerate. However, Zeeman data reported in this work conclusively demonstrate that  $g \leq 0.04$  (implying  $\langle L_z \rangle \approx 0$ ). Therefore, either these transitions involve orbitally non-degenerate excited states or degenerate excited states in which the  $z$  component of orbital angular momentum is quenched. Stark experiments can discriminate between these two possibilities.

#### 4.1. Stark results and orbital degeneracy

In order to use the presented Stark effect data for regions I and II to determine the nature and symmetry of the excited states involved in these transitions, it is necessary to consider, in some depth, the above two possibilities. If, as earlier workers have claimed [1, 2–5, 8, 12–15], observed Stark effects are due to splitting of orbitally degenerate states by an electric field applied parallel to the molecular plane ( $E \perp c$ ), this splitting should be independent of external field orientation in the molecular plane. Thus, if  $E$  is rotated about the  $c$  axis in the 4.2°K sym-triazine crystal, Stark splitting patterns should be constant\*. On the other hand, if the transitions in question involve orbitally non-degenerate states, the Stark pattern would be highly in-plane angle dependent. There are then expected to be considerable changes in Stark splittings as the crystal is rotated about the  $c$  axis in a constant intensity  $E \perp c$  applied field.

While the above is straightforward, exactly what changes in Stark splitting are expected as  $E_{\perp}$  is rotated in the molecular plane depend crucially upon quality

\* (i) Such experiments were attempted using ac fields because sample-electrode contact could not be maintained. Large variations, in part due to sample-field rotation difficulties and artifacts and in part due to in-plane angle dependence of Stark patterns, were observed. Since it was difficult to separate these two effects, we abandoned the approach.

(ii) This assumes that the phase transition does not tilt molecular planes so that they are no longer perpendicular to the stacking direction. Such tilting would introduce an orientational Stark effect of order  $(1 - \cos \alpha)$ , where  $\alpha$  is the tilt angle. Since  $\alpha < 2-3^\circ$  (ref. [10]), this effect cannot amount to more than 1%. Further, since the  $c$  axis of the  $R\bar{3}c$  room temperature crystal and the monoclinic low temperature crystal coincide [10], the  $c$  axes of the three twins also coincide.

of the room temperature crystals. To illustrate this point, and explain the data, two limiting cases are presented below.

*Case 1:* The room temperature crystal is of reasonably good quality; it may contain microscopic flaws, fault planes, etc., but all regions of the crystal are composed of stacks of molecules whose planes are perpendicular to  $c$ . Moreover, suppose that all stacks of molecules throughout the bulk crystal are *in phase*, such that there is a unique *macroscopic* direction  $X(\perp c)$ , such that any vector passing through a molecular center, parallel to  $X$  bisects a C–N bond.  $\pi/2$  from  $X$  there is a  $Y(X \perp Y \perp Z \parallel c)$  such that any vector parallel to  $Y$  passing through a molecular center intersects an atom. It is further assumed that the states involved do not have crystal-fixed electric dipole moments in the room temperature site.

When such a crystal passes through the phase transition at 213°K [10], a dipole moment will be induced in each molecule in a unique and crystal fixed direction. For each of the three components of the triply-twinning macroscopically ordered sample, molecular (site) dipole moments will be aligned along one distortion-fixed direction. Since, however, the directions of the three twin sections are disposed at  $2\pi/3$  to each other, the resultant bulk crystal will have an equal number of molecules with dipole moments distortion aligned in three directions differing by  $2\pi/3$  in a plane perpendicular to the monoclinic (also  $R\bar{3}c$ )  $c$  axis. With the crystal  $c$  axis parallel to the molecular  $Z$  (out-of-plane) axis, the plane of these dipole moments is approximately the molecular ( $D_{3h}$ ) plane. If it is assumed that the monoclinic phase (like  $R\bar{3}c$ ) has 2 molecules/unit cell related by inversion or a plane (that is, a space group isomorphic to  $C_{2h}$ ), then for each dipole oriented along a given direction, there is another oriented  $\pi$  with respect to it. The resultant "bulk crystal dipole pattern" has approximate six-fold symmetry and is depicted in fig. 12. A space group isomorphic to the  $C_5$  point group, with particular and severe restriction, yields the same results.

With an external electric field applied perpendicular to a "side" of the resultant "hexagonal" pattern, expected Stark patterns contain 3 maxima (fig. 12,  $\theta = 0^\circ$ ). But with  $E$  applied such that it intersects a "vertex" of this hexagonal array, an apparently "normal" 2 maxima Stark pattern obtains (fig. 12,  $\theta = 30^\circ$ ). Figs. 13 and 14 show, respectively,  $\theta = 0^\circ$  and  $\theta = 30^\circ$

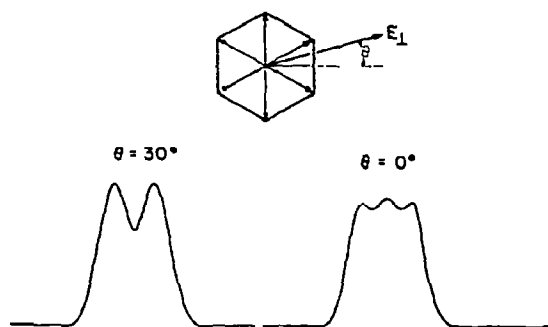


Fig. 12. Expected high field Stark pattern for an orbitally non-degenerate transition in a "case 1" crystal. The hexagonal bulk crystal dipole moment pattern is also shown as discussed in the text. The absorption patterns were plotted by computer using the formula:  $I = \sum_{j=1}^6 I_0 \exp[-(x - P_j)^2 / W^2]$ , where  $P_j = S \cos[60(j) - \theta + 30]$ .

computer plotted line shape patterns as a function of field intensity.

*Case 2:* The room temperature crystal is so highly flawed that stacks of molecules in various regions of the bulk sample have lost all (in-plane) phase relation with respect to one another. Although all stack axes may still be in the  $c$  ( $Z$ ) axis direction, and in-plane

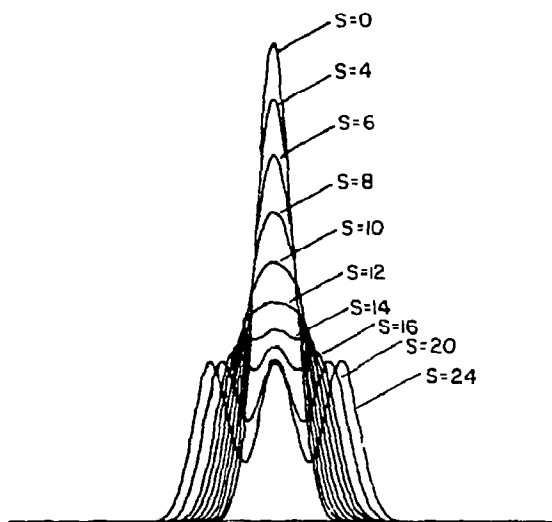


Fig. 13. Field dependence of the  $\theta = 0^\circ$  lineshape.  $W = 8$ ,  $I_0 = 40$  (see fig. 12).

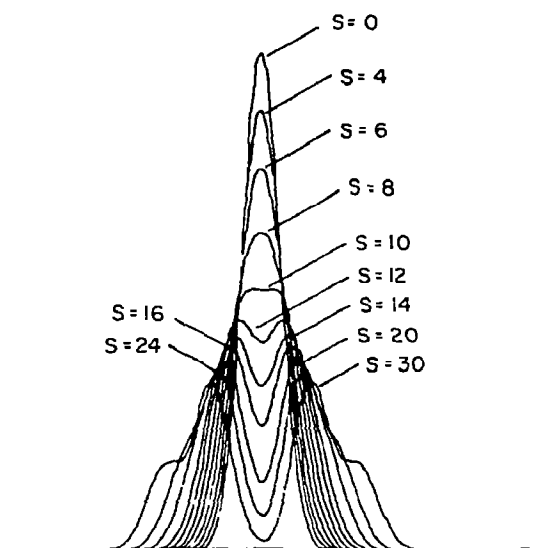


Fig. 14. Field dependence of the  $\theta = 30^\circ$  lineshape.  $W = 8$ ,  $I_0 = 40$  (see fig. 12).

ordered domains may exist, there is no macroscopic direction which is purely "through bonds" or "through atoms". When such a crystal cools below the phase transition, the resultant crystal induced dipole pattern is completely random. Fig. 15 presents a computer plotted Stark splitting line shape for this completely averaged situation. The pattern evidences only two maxima even in the limit of arbitrarily high applied fields.

While the random dipole pattern is invariant with respect to rotation of the applied field about the  $c$  axis, it nonetheless differs from that expected for an orbitally degenerate transition in overall splitting, width, and line shape. This is clearly seen by comparing figs. 8, 12–15.

DC Stark results reported in section 3 show that regions I and II involve orbitally non-degenerate states. Observed high field Stark patterns (figs. 9–11) are precisely those expected for a transition to an orbitally non-degenerate state in a case 1 crystal  $\theta \approx 0^\circ$ . A further confirmation that excited states corresponding to region I and II absorptions of all isotopic species are orbitally non-degenerate comes from the superimposability of  $C_{2v}$  and  $D_{3h}$  isotope Stark patterns (figs. 6, 9–11).

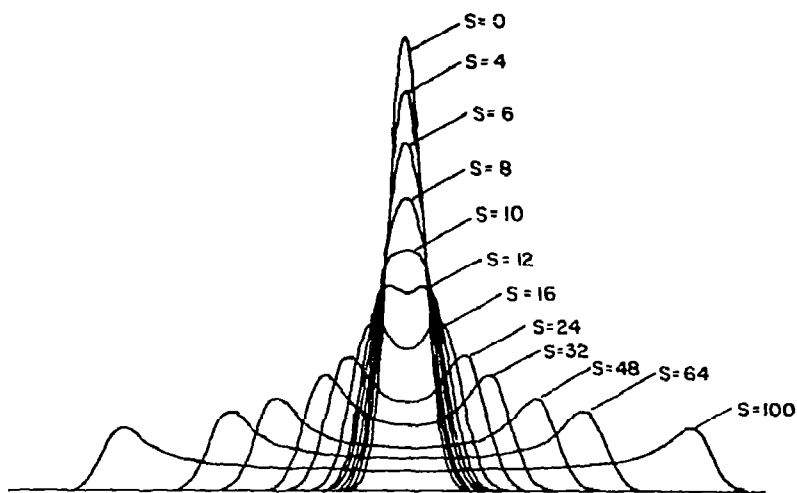


Fig. 15. Field dependence for the averaged (case 2) lineshape.  $W = 8$ ,  $I_0 = 40$  (see fig. 12).

Since there no longer appears to be any compelling and viable alternative explanation for these Zeeman, Stark and  $C_{2v}$  isotope absorption results, the sym-triazine 4.2°K crystal spectra will be assigned on the basis that excited states associated with region I and II transitions are orbitally *non*-degenerate.

#### 4.2. Assignment of region II

Gas phase absorption [6, 16] and fluorescence [17] spectra of region II ( $\pm 1000 \text{ cm}^{-1}$ ) have been assigned as  ${}^1E'' \leftarrow {}^1A_1'$ . With the exception of hot bands, both crystal and gas phase transitions are quite similar. Particularly noteworthy is that  $h_3$ - and  $d_3$ -sym-triazine origins in both gas and crystal are separated by  $118.8 \pm 0.4 \text{ cm}^{-1}$ . Also, region II absorption in trioxane crystals (see part I) gives virtually identical isotope differences. It is thus highly probable that the same  ${}^1E'' \leftarrow {}^1A_1'$  transition is responsible for the observed spectra in all three environments.

These facts, taken with present Stark, Zeeman, and absorption crystal data, make it reasonable to assign region II absorption to *one component* of a crystal field split  ${}^1E'' \leftarrow {}^1A_1'$  transition.

#### 4.3. ${}^1E'' \leftarrow {}^1A_1'$ spectra of $C_{2v}$ isotopes

Perhaps the most striking feature of region II spectra of isotopic mixed crystals of sym-triazine is the fact that there are two transitions for each  $C_{2v}$  symmetry isotopic species but only one for each  $D_{3h}$  symmetry isotope. For deuterated  $C_{2v}$  isotopes, splitting of the  ${}^1E'' \leftarrow {}^1A_1'$  absorption is  $25.0 \text{ cm}^{-1}$  (see part I).

A smaller but entirely similar effect has been observed for the  ${}^1B_{2u}, {}^3B_{1u} \leftarrow {}^1A_{1g}$  transitions of benzene [18, 19]. The explanation proposed to account for this "anomalous splitting" of low symmetry isotope spectra [18] is quite convincing and applies equally well to sym-triazine. In this explanation, the multiplet pattern is seen as a consequence of a crystal-field induced, static distortion of the molecule into a lower symmetry configuration. Of course, this distortion is completely independent of isotopic composition and position of isotopic substitution. As a result of such a distortion, the three carbon atoms in sym-triazine, for instance, are no longer equivalent. The C-H vibrational force constants are, therefore, no longer equivalent for the three positions on the distorted ring. Substitution of D for H will result in a position-dependent change in molecular zero point energy. That is, the molecular zero point energy becomes a function of isotopic substitution with respect

to the independent crystal induced distortion. Similar effects are expected for  $^{15}\text{N}$  or  $^{13}\text{C}$  substitution in the molecular ring (see part I). Although magnitude of the effect should be less for  $^{13}\text{C}$  or  $^{15}\text{N}$  due to the much smaller relative mass change involved, the change in ring (C–N) force constants should be larger than for C–H force constants.

As a result of this zero point energy variation, optical spectra of the various positional isomers of a particular isotope will be displaced relative to each other by an amount equal to the difference in the zero point energy changes for electronic transitions of the isomers. Magnitude of the observed "anomalous splitting" in spectra of these isotopes is, therefore, an indirect measure of the magnitude of the molecular distortion. If distortions of the ground and excited states are similar, only very small splittings are expected since the zero point changes in the two states tend to cancel. If, however, one of the states is particularly susceptible to a distortion in a low symmetry field, zero point differences will not cancel and a sizable splitting of the asymmetric isotope absorption due to inequivalent positional isomers is expected. For convenience we will call this positional isomer energy difference in the distorted molecule the *zero point orientational splitting* (ZPOS).

One of the main consequences of Jahn–Teller (JT) and pseudo-Jahn–Teller (PJT) effects is that the associated molecular electronic states become very sensitive to stress applied in certain directions (see, e.g., [20]). Large ZPOS are therefore expected in spectra of asymmetric isotopes for which JT or PJT forces are operative. For benzene, the ZPOS is more than three times larger in the  $^3\text{B}_{1u}$  state than in the  $^1\text{B}_{2u}$  state [18, 19]. The splitting in the triplet state amounts to about  $7\text{ cm}^{-1}$  for  $\text{C}_6\text{H}_5\text{D}$  and  $14\text{ cm}^{-1}$  for  $p\text{C}_6\text{H}_4\text{D}_2$ . This increased susceptibility to distortion displayed by  $^3\text{B}_{1u}$  may well be a direct consequence of the strong PJT coupling of this state to the JT active  $^3\text{E}_{1u}$  [18, 21–23].

In sym-triazine, ZPOS of the  $d_2h_1$  and  $d_1h_2$  isotopes in region II is more than three times larger than the  $^3\text{B}_{1u}$  and more than an order of magnitude greater than the  $^1\text{B}_{2u}$  state of benzene. Unfortunately these benzene data apply only to benzene in the  $\text{C}_i$  site of a benzene crystal, and the corresponding ZPOS in a triazine crystal is, of course, unknown. A rough calibration may be obtained by comparison of the splitting

of the  $\nu_6(e_{2g})$  degenerate ground state benzene crystal vibration ( $3.1\text{ cm}^{-1}$ ) [19] with the splitting of  $\nu_6(e'_1)$  ground state sym-triazine crystal vibration ( $\sim 7\text{ cm}^{-1}$ ) [24]\*. In a sym-triazine crystal at  $4.2^\circ\text{K}$  one might therefore expect a ZPOS in asymmetrical isotopes of sym-triazine in a "normal" (non-JT or non-PJT active) electronic state to be of the order of twice that of the  $^1\text{B}_{1u}$  state of a benzene crystal, i.e.,  $2 \times (< 2\text{ cm}^{-1}) \leq 4\text{ cm}^{-1}$ .\*\* The observed ZPOS of  $25.0\text{ cm}^{-1}$  is more than six times larger than one might expect for a non-JT or a non-PJT active state. This argument then favors assignment of region II to a transition involving the  $^1\text{E}''$  state which, because of the JT effect, is rendered highly susceptible to distortion by asymmetric crystal fields.

#### 4.4. Assignment of region I

The fact that the  $\text{C}_{2v}$  isotopes of sym-triazine show region I absorptions split by  $30\text{ cm}^{-1}$  (see part I) with intensity and Stark pattern identical to those of region II transitions indicates that the excited state associated with region I is even more distortable than that of region II. Region I is therefore assigned as *one component* of the  $^3\text{E}'' \leftarrow ^1\text{A}'_1$  transition split by the low symmetry crystal field. The molecule in a  $^3\text{E}''$  state has probably been rendered highly sensitive to such a distortion by the Jahn–Teller effect.

This assignment is further strengthened by the following three points:

(1) The  $^3\text{E}''$  state is expected to lie lowest, particularly in the case where  $^1\text{E}''$  is the lowest singlet state [9].

(2) The  $^3\text{E}''$  state has been assigned to lie lowest in the gas as an explanation for no observed phosphorescence under conditions which were ideal for its observation [17]. The  $^3\text{E}''$  state is directly and strongly spin–orbit coupled to the ground state, thus providing a uniquely good radiationless relaxation path [13, 15].

\* The  $\nu_6$  vibrations of the two molecules are only approximately comparable. In the lower symmetry of sym-triazine the  $e_{2g}$  and  $e_{1u}$  vibrations of benzene can be expected to be somewhat mixed.

\*\* This is an upper bound. Benzene in borazine gives  $\Delta(^1\text{B}_{2u})/\Delta(^3\text{B}_{1u}) < 0.2$  with ZPOS for  $^1\text{B}_{2u}$  still  $< 4\text{ cm}$  for  $\text{C}_6\text{H}_5\text{D}$  [25].

(3) The  ${}^3E''$  state as the lowest triplet state in the solid would explain a quantum yield for phosphorescence of less than  $10^{-9}$  [9]. If  ${}^3A_1''$  were lowest (or  ${}^3A_1'$ , for that matter), it is hard to understand why phosphorescence would be so weak.

#### 4.5. Geometry in the ${}^1E''$ and ${}^3E''$ excited states in the crystal

The observation of only two absorption lines, whose intensity differ by a factor of  $\sim 2$ , for each  $C_{2v}$  isotope,  $d_1h_2$  and  $d_2h_1$ , in the  ${}^1,3E'' \leftarrow {}^1A_1'$  transitions, suggests that the molecular symmetry in the 4.2°K crystal is approximately  $C_2$  (or, less likely,  $C_s$ ). If the simple model for ZPOS postulated in ref. [18] is imposed on sym-triazine, one finds that the lowest observed singlet and triplet states must be distorted in a sense opposite to that of the  ${}^3B_{1u}$  benzene state in a benzene crystal. This is a direct and straightforward consequence of the fact that for  $h_2d_1$ -sym-triazine the lower energy line is more intense, while for the  $h_1d_2$ -sym-triazine isotope the higher energy line is more intense (figs. 6b, 9–11 of part I; see also fig. 3 above). Since distortion of the benzene triplet has been determined to be “anti-quinoidal” (that is, two long bonds and four short bonds) [18, 22], distortion of the lowest singlet and triplet states of sym-triazine must be “quinoidal” (four long bonds and two short bonds).

#### 4.6. Location and identity of the components of the split ${}^1,3E''$ states

When a degenerate E electronic state is split by a crystal field, the Jahn–Teller coupling of these states is replaced by a pseudo Jahn–Teller coupling that diminishes in intensity as the energy separation between the components increases. In the limit of very large splitting (much greater than the frequency of a typical vibrational mode), the two components of an E state can be expected to behave independently as well-isolated, adiabatic states of the distorted molecule. It is quite important, therefore, to locate the other component of the E state so that some measure may be had of the residual vibronic coupling between these states.

Upon distortion of the  $D_{3h}$  molecule to  $C_2$  symmetry, an  $E''$  state will split into two states, one trans-

forming as A, the other as B in the  $C_2$  point group (see fig. 16). The A component of  $E''$  will mix with other  $D_{3h}$  sym-triazine states which transform as A in  $C_2$  and through this mixing it will obtain E1 allowed character polarized uniquely along the y axis of the molecule (we will continue to use the  $D_{3h}$  axis system as shown in fig. 16 for this discussion). On the other hand, the B state will gain both x and z polarized E1 intensity and will therefore exhibit a mixed electric dipole polarization. Since region II absorption in sym-triazine exhibits  $\sim 70\%$  in-plane polarization and  $\sim 30\%$  out-of-plane polarization [2], it would be natural to assume that region II therefore corresponds to the B component of the E state. The A component can be expected to be E1 polarized more uniquely in-plane and to have an absorption intensity no less than 60–70%

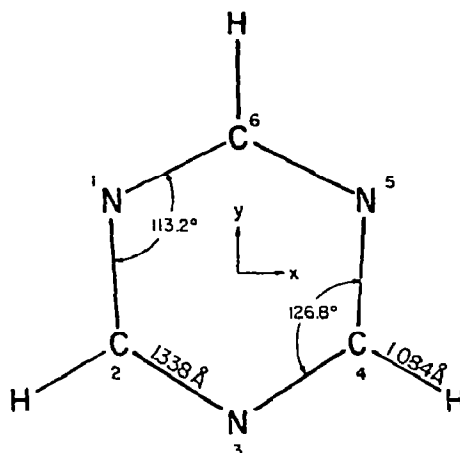


Fig. 16a. Equilibrium ground state geometry of sym-triazine.

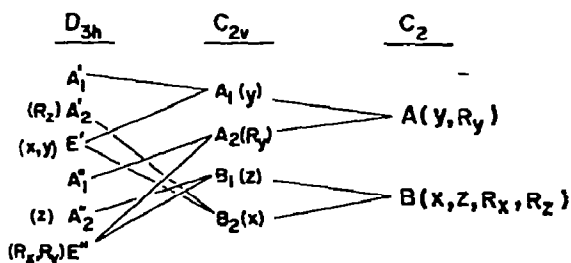


Fig. 16b. Correlation between the point groups  $D_{3h}$ ,  $C_{2v}$  and  $C_2$ .

of that of region II. Of course, both states can exhibit magnetic dipole intensity, which would give them an apparent mixed E1 intensity; indeed, the mixed polarization of region II has been used to assign M1 activity to this feature. It is in principle straightforward to separate E1 and M1 intensity patterns by following intensity as a function of angle over the sphere. However, in a biaxial monoclinic crystal this would be technically extremely difficult and probably quite inaccurate. It is far from simple to account quantitatively for the large effects of linear birefringence away from the optic axes of a biaxial crystal [26]. The unique choice of an A or B state for region II is not possible with the present data.

The triplet state (region I) Zeeman intensity pattern, as has been previously noted in I and ref. [15], is different than that expected and found for other aromatic azines. At  $H \neq 0$  the  $\tau_z$  spin component is about a factor of 6 more intense than the  $\tau_x$  and  $\tau_y$  spin components. In ref. [15] it is stated that the main azine spin-orbit coupling intensity enhancement route ( ${}^1E' \rightarrow {}^3E''$ ), which brings radiative intensity to in-plane spin components, is suppressed in  $D_{3h}$  symmetry. Any  $z$  polarization or intensity at the origin implies an  $n\pi^* \rightarrow \pi\pi^*$  spin-orbit coupling and should in general be quite small. However, in  $C_2$  (or lower) symmetry, with relatively large vibronic and crystal field mixing, the intensity patterns become much less difficult to rationalize. The dominant  $\tau_z$  component intensity and the weak  $\tau_x, \tau_y$  component intensity might well arise from a still mostly suppressed ( ${}^1E' \rightarrow {}^3E''$ ) route and a distortion enhanced ( ${}^1A_2' \rightarrow {}^3E''$ ) route (see fig. 16). If it is assumed that the mechanism for this pathway involves only spin-orbit coupling, then region I can be assigned (based on the Zeeman intensity patterns) as A in  $C_2$  symmetry. However, if spin-orbit vibronic coupling is prevalent in this crystal field distorted Jahn-Teller active origin, then either A or B symmetry is clearly possible.

While regions I and II are probably either both A or both B symmetry site states, it is premature to pick one because of difficulty with polarizations and possibility of spin-vibronic intensity at the  ${}^3E'' \leftarrow {}^1A_1'$  origin.

Upon examination of pure crystal spectra it is evident that the two components of  ${}^1E'' \leftarrow {}^1A_1'$  must be separated by at least  $198 \text{ cm}^{-1}$ . Region III absorption in the pure crystal (see part I) has no obvious

counterpart in gas phase absorption spectra [6] and it is therefore a natural choice for the other component of the crystal-field split  ${}^1E''$  state. However, the *main peak* in region III does not exhibit an observable ZPOS for  $C_{2v}$  isotopes [1, 9]. This main peak in region III, therefore, is not likely the other component of the  ${}^1E''$  state.

The broad absorption in region III may obscure the other component of the  ${}^1E''$  state. It is also possible that peaks higher in energy than region III might be associated with the other component of the  ${}^1E''$  state (see part I). However, all peaks from 200 to  $700 \text{ cm}^{-1}$  higher than region II show isotope shifts which are compatible with their assignment to vibrations built on the region II origin [6]. The spectrum above  $700 \text{ cm}^{-1}$  is too broad and complex for interpretation at present.

With current data, therefore, it is not readily possible to locate the other component of the split  ${}^1E''$  state. It is probable, however, that this other component is split away from the region II origin by at least  $200 \text{ cm}^{-1}$ . Region I also has such a feature  $185 \text{ cm}^{-1}$  to higher energy but these absorptions are even broader and more difficult to analyze than region III.

#### 4.7. Some implications of these assignments

The single most important difficulty in studying sym-triazine in the solid state is that the quantum yield for luminescence is so exceedingly small that no positively identifiable emission from sym-triazine has been detected under conditions which are nearly ideal for its observation [9]. In the lowest singlet state, some responsibility for low fluorescence quantum yield must be borne by the extremely low radiative strength of the transition. However, if  ${}^3E' \leftarrow {}^1A_1'$  is the  $T_0 \leftarrow S_0$  transition, the low quantum yield for phosphorescence must be due to a particularly facile non-radiative process. There are two possible major explanations for extraordinarily active radiationless relaxation processes in sym-triazine.

(1) Distortion of the excited state: It is known from ZPOS of  $C_{2v}$  isotope features and the Stark effect that the excited states involved are measurably distorted in the crystal. This distortion can be expected to increase the (Franck-Condon) overlap with nearly isoenergetic, high quantum number ground state vibrations and thus enhance internal conversion to the ground state

(2) Spin-orbit coupling routes and radiationless transitions: Since regions I and II correspond to crystal field split  $1^3E'' \leftarrow 1A_1'$  transitions, spin-orbit coupling rationalizations [13, 15] offer a particularly convincing explanation for lack of emission from sym-triazine in the solid state. This explanation requires that the  $3A_1' (\pi\pi^*) \leftarrow 1A_1'$  transition lies within the  $1079 \text{ cm}^{-1}$  gap between  $3E'' \leftarrow 1A_1'$  (region I) and  $1E'' \leftarrow 1A_1'$  (region II) transitions. This is a reasonable assumption since: (a)  $3A_1'$  is predicted to be nearly isoenergetic with  $3E''$ ; (b) the absorption spectrum in this region is dramatically broadened just as would be expected if the unobserved  $3A_1'$  state were strongly coupled to overlapping  $3E''$  vibronic states in this region [27]; and (c) the analogue of the  $3A_1' \leftarrow 1A_1'$  transition is found below the  $S_1$  state in both pyrazine [28] and pyrimidine [28, 29].

It is expected that, as in other azines, absorption into any part of the sym-triazine crystal spectrum higher in energy than region II will form crystal excitations which rapidly undergo radiationless relaxation to the (split)  $1E''$  state. Quantum yield for fluorescence from  $S_1$  will be quite small since the radiative transition is so weak and because very strong one-center spin-orbit coupling exists between the  $1E''$  state and the  $\tau_x, \tau_y$  sublevels of the  $3A_1'$  state. This in turn populates, through radiationless relaxation, the  $\tau_x, \tau_y$  sublevels of the  $3E''$  state. But, these sublevels are strongly (and non-radiatively) spin-orbit coupled to the ground state [13, 15]. The abnormally low quantum yield of both fluorescence and phosphorescence at low temperature are thereby simply explained by this model. At temperatures for which the spin-lattice rate constant might compete with the  $\tau_x, \tau_y$  radiationless rate constant to the ground state, other mechanisms associated with energy transfer and exciton-phonon coupling, tend to limit the radiative efficiency of triplet states.

To the extent that this latter explanation actually accounts for the difficulty of observing phosphorescence from sym-triazine, such difficulty can be easily overcome. Note that it is the  $\tau_z$  spin component of the  $3E''$  state that is radiatively well coupled to the ground state. At sufficiently low temperatures such that spin-lattice relaxation times are  $> 1$  sec, any population of the  $\tau_z$  sublevel of the  $3E''$  state can be expected to have a high quantum yield for phosphorescence. The unfortunate circumstance for sym-triazine

is that, if the  $3A_1' (\pi\pi^*)$  state is lower than the  $1E'' (\pi\pi^*)$  state, effectively no population of the  $\tau_z$  level of  $3E''$  can be expected to result from excitation into the singlet manifold. There are, however, at least two ways of producing  $\tau_z$  population in  $3E''$ :

Method 1: The zero-field EPR transitions between the  $\tau_z$  and  $\tau_x, \tau_y$  sublevels can be saturated under conditions of continuous UV irradiation at  $\lambda < 3300 \text{ \AA}$ . Populations in these triplet levels will thus be equalized and radiative quantum yields will go up in proportion to the increase in radiative transition moment. High field Zeeman data show that the relative transition moment for the  $\tau_z$  as compared to the  $\tau_x, \tau_y$  levels is  $\sim 6$  to  $1$  [3, 5, 12]. Therefore, a six-fold increase in phosphorescence quantum yield is expected with this technique. Much larger phosphorescence quantum yield enhancements can be obtained by pulsed or adiabatic passage techniques which invert the level population.

Method 2: The  $\tau_z$  sublevel of the  $3E'' (T_1)$  state can be populated by direct excitation into the region I absorption of a sym-triazine crystal. This technique would require a laser, but it is virtually assured of success if the foregoing assumptions are correct. The enhancement of phosphorescence intensity could be many orders of magnitude.

Of course, the assumptions used above may not apply since they are strictly valid only for the  $D_{3h}$  and to some extent  $C_{2v}$  symmetry molecule. In the  $C_2$  symmetry situation actually present in the low temperature crystal, the  $\tau_z$  spin sublevel may also be spin-orbit coupled to the ground state, in which case a more modest enhancement of the overall phosphorescence quantum yield would obtain by direct region I excitation.

There is one piece of experimental data that tends to substantiate belief that the above methods may work: the phosphorescence (impurity?) excitation efficiency for isotopic mixed crystals of sym-triazine [9] was observed to be more than a factor of ten greater for direct excitation into  $3E'' \leftarrow 1A_1'$  than for excitation into  $1E'' \leftarrow 1A_1'$ . Excitation experiments with high power lasers may therefore be quite fruitful in this regard. We plan such experiments with output from a doubled or non-linearly mixed dye laser in the near future.

## 5. Summary

All data (Stark, Zeeman, Stark–Zeeman,  $C_{2v}$  isotope absorption) indicate that regions I and II must each be assigned as one component of Jahn–Teller-sensitized, crystal-field split  ${}^3E'' \leftarrow {}^1A_1'$  and  ${}^1E'' \leftarrow {}^1A_1'$  transitions, respectively. From zero point orientational splittings (ZPOS) for  $C_{2v}$  isotopes it has been determined that the excited states associated with these transitions in a  $4.2^\circ\text{K}$  (monoclinic) sym-triazine crystal are distorted into a quinoidal geometry (i.e., two short bonds and four long bonds).

## References

- [1] E.R. Bernstein and R.E. Smalley, *J. Chem. Phys.* 58 (1973) 2197 (referred to as I).
- [2] R.M. Hochstrasser, T.S. Lin and A.H. Zewail, *J. Chem. Phys.* 56 (1972) 637.
- [3] R.M. Hochstrasser and A.H. Zewail, *J. Chem. Phys.* 55 (1971) 5291.
- [4] R.M. Hochstrasser and A.H. Zewail, *Chem. Phys. Letters* 11 (1971) 157.
- [5] R.M. Hochstrasser and T.S. Lin, *Symp. Faraday Soc.* 3 (1969) 100.
- [6] G. Fischer and G.J. Small, *J. Chem. Phys.* 56 (1972) 5934.
- [7] G. Fischer, *J. Chem. Phys.* 57 (1972) 2646.
- [8] D.A. Wiersma, *Chem. Phys. Letters* 16 (1972) 517.
- [9] R.E. Smalley, Ph.D. Thesis, Princeton University (1973).
- [10] P. Coppens and T.M. Sabine, *Mol. Cryst.* 3 (1968) 507; *P. Coppens, Science* 158 (1967) 1577.
- [11] R.M. Hochstrasser, *Chem. Phys. Letters* 21 (1973) 15, and private communication.
- [12] T.J. Aartsma and D.A. Wiersma, *Chem. Phys.* 1 (1973) 211, and private communication.
- [13] R.M. Hochstrasser, *Chem. Phys. Letters* 15 (1972) 316.
- [14] R.M. Hochstrasser, *Mol. Phys.* 24 (1972) 597.
- [15] R.M. Hochstrasser, *Chem. Phys. Letters* 17 (1972) 1.
- [16] J. Barnard, J.R. Christie and J.E. Parkin, to be published and private communication.
- [17] A.E.W. Knight and C.S. Parmenter, *Abstract  $\Delta 2$ , 28th Symp. Mol. Structure and Spectroscopy, The Ohio State University* (1973), and private communication.
- [18] G.C. Nieman and D.S. Tinti, *J. Chem. Phys.* 46 (1967) 1432.
- [19] E.R. Bernstein, S.D. Colson, D.S. Tinti and G.W. Robinson, *J. Chem. Phys.* 48 (1968) 4632.
- [20] R. Englman, *The Jahn–Teller effect in molecules and crystals* (Wiley–Interscience, New York, 1972) p. 1 ff.
- [21] D.M. Burland, G.C. Castro and G.W. Robinson, *J. Chem. Phys.* 52 (1970) 4100.
- [22] A.M. Ponte-Goncalves and C.A. Hutchison Jr., *J. Chem. Phys.* 49 (1968) 4235.
- [23] J.H. van der Waals, A.M.D. Berghuis and M.S. de Groot, *Mol. Phys.* 21 (1971) 497.
- [24] D.M. Hanson, private communication.
- [25] S.D. Colson and J.M. van Pruysen, private communication.
- [26] M. Born and E. Wolf, *Principles of optics* (Pergamon Press, London, 1959) Ch. XIV.
- [27] R.M. Hochstrasser and C.A. Marzocco, *J. Chem. Phys.* 49 (1968) 971; *Molecular luminescence*, ed. E.C. Lim (Benjamin, New York, 1969) p. 631 ff.
- [28] D.M. Burland and J. Schmidt, *Mol. Phys.* 22 (1971) 19.
- [29] Y. Chan and M. Sharnoff, *J. Luminescence* 3 (1970) 155.